

# Suppressing the classical noise in the accelerated geometric phase gate by optimized dynamical decoupling

Da-tong Chen<sup>1</sup> and Jun Jing<sup>1,\*</sup>

<sup>1</sup>*School of Physics, Zhejiang University, Hangzhou 310027, Zhejiang, China*

In the quantum computation scenario, geometric phase-gates are becoming increasingly attractive due to their supposed intrinsic fault tolerance. In an adiabatic cyclic evolution, Berry phase appears to realize a geometric transformation. Performing the quantum gates as many as possible within the timescale of coherence, however, remains an inconvenient bottleneck due to the systematic errors. Here we propose an accelerated adiabatic quantum gate based on the Berry phase, the transitionless driving, and the dynamical decoupling, which reconciles a high fidelity with a high speed in the presence of control noise or imperfection. We optimize the dynamical-decoupling sequence in the time domain under a popular Gaussian noise spectrum following the inversely quadratic power-law.

## I. INTRODUCTION

By processing the data in a quantum-mechanical way, quantum computation out-performs its classical counterpart in selected algorithms or tasks [1, 2]. The simulation of the coherent evolution of generic quantum systems can be modelled by orderly performing sequences of high-fidelity unitary operations [3–5]. The ubiquitous noises from uncontrollable environment and imprecise control, however, are inevitable in any experimental proposal, which pose challenges to the quality of quantum gate in terms of fidelity and operation time [6, 7]. The quantum geometric phase [8–12], which is accumulated when the system is moving in the parameter space, has intrinsic tolerant property and is robust against certain fluctuations during the trajectory. The geometric quantum computation is therefore appealing and becoming feasible in many experimental platforms, including the trapped ions [13, 14], the nuclear magnetic resonance [15, 16], and the superconducting circuits [17, 18].

As a benchmark implementation of the Abelian geometric transformation, the quantum gate based on the Berry phase requires that the quantum system undergoes a desired adiabatic loop in the parameter space [8]. The process is intrinsically slow. In practice, reducing the evolution time is demanded to avoid the accumulation of the decoherence influence. On the other hand, however, speeding up always gives rise to the transition between the instantaneous eigenstates of system, which is supposed to be “frozen” in the adiabatic condition to maintain the gate fidelity. So that the competitive decoherence time and the high fidelity are seemingly contradictory for the adiabatic geometric quantum gates. One of the compromise solutions to reduce the evolution time is using the quantum gates based on the Aharonov-Anandan phase [9, 19], which emerges in arbitrary cyclic unitary evolutions. Alternatively, one can accelerate the evolution process via the approach of the transitionless quantum driving (TQD) [20], which is formulated by the

corrected Hamiltonian to avoid the level crossing during the time evolution.

The TQD-accelerated quantum gate based on the Berry phase is still sensitive to the systematic errors in the control Hamiltonian or driving parameters. A significant feature of geometric quantum computation is its compatibility with certain error-suppression techniques to maintain the fidelity of the unitary transformation, e.g., the dynamical decoupling (DD) [21–25], the unconventional geometric gates [26–28], the decoherence-free subspaces [29], and the quantum error correction in holonomic quantum computation [30, 31]. The dynamical decoupling was originated in the high-precision magnetic resonance spectroscopy and has been applied to the field of quantum control as a long standing technique. A typical DD is to neutralize the effects from the fluctuation noises by applying a sequence of inverse operations to a two-level system [21]. In this work, we aim to find an optimized dynamical-decoupling sequence to protect the TQD-accelerated Berry-phase gate.

Particularly, we consider the effect from the Gaussian stochastic noises [32] in the control parameters of our nonadiabatic geometric quantum gates, which would deviate the output states from the noise-free situation. Under various resource of noises, we analysis the robustness of the gate-fidelity for a general input state to estimate the deviation and then apply the dynamical-decoupling sequences to improve the fidelity. In the time domain, we analytically derive an optimized DD sequence under the Gaussian color noise following the inversely quadratic power-law spectrum.

The rest of the work is arranged as follows. In Sec. II, we start from a semi-classical Rabi model under parametric driving and obtain a general time-dependent qubit Hamiltonian corrected by the counter-rotating interaction up to the first order. This Hamiltonian is used to establish a set of more accurate Berry phase gates accelerated by the transitionless quantum driving. In Sec. III, we consider the stochastic fluctuations in various control parameters and their damages to the fidelity of the preceding nonadiabatic transformation in the free induction decay (FID). Then in Sec. IV, we propose a scheme to apply the DD technique to the Berry phase gate and discuss

\* [jingjun@zju.edu.cn](mailto:jingjun@zju.edu.cn)

the results under the inversely quadratic noise spectrum. The detailed derivation of the optimized control sequence can be found in Appendix A. We summarize the whole work in Sec. V.

## II. A MORE ACCURATE EFFECTIVE HAMILTONIAN

We start with a Rabi model under parametric driving, where a two-level system (qubit) with energy-spacing  $\omega_a$  is controlled by a driving field with time-modulated frequency  $\omega_b(t)$  and phase factor  $\varphi_R(t)$ . The strength of the dipole-dipole interaction between the qubit and the driving field (Rabi-frequency) is described by  $\Omega_R(t)$ . The system Hamiltonian thus can be written as

$$H(t) = \frac{\omega_a}{2}\sigma_z + \Omega_R(t) \cos[\Omega_b(t) + \varphi_R(t)]\sigma_x, \quad (1)$$

where  $\Omega_b(t) \equiv \int_0^t ds \omega_b(s)$ . It is not easy to construct a stable quantum gate directly from this original Hamiltonian in Eq. (1) for the lack of an analytical solution. It is popular to see the application of the rotating-wave approximation (RWA) in the previous treatments [14, 33, 34]. With respect to the unitary transformation  $R(t) = \exp[i\Omega_b(t)\sigma_z/2]$ , one can find

$$\begin{aligned} H'(t) &= R(t)H(t)R^\dagger(t) + i\dot{R}(t)R^\dagger(t) \\ &= \frac{1}{2}\{[\omega_a - \omega_b(t)]\sigma_z \\ &\quad + \Omega_R(t)[\cos\varphi_R(t) + \cos(2\Omega_b(t) + \varphi_R(t))]\sigma_x \\ &\quad + \Omega_R(t)[\sin\varphi_R(t) - \sin(2\Omega_b(t) + \varphi_R(t))]\sigma_y\} \\ &\approx \frac{\omega_a - \omega_b(t)}{2}\sigma_z + \frac{\Omega_R(t)}{2}\left[e^{-i\varphi_R(t)}\sigma_+ + h.c.\right], \end{aligned} \quad (2)$$

where the terms oscillating with the frequency  $2\Omega_b(t)$  are omitted. The error between the resultant Hamiltonian under RWA and the original one is thus in the first order of  $\mathcal{O}(\Omega_R)$ .  $H'(t)$  applies to the dispersive regime of a sufficiently weak driving strength. The contribution of the omitted counter-rotating terms becomes however significant in the strong-coupling regime and demonstrates intriguing dynamical behaviors [35–38].

To retain the first-order contribution from the counter-rotating terms, we choose a different approach with a modified rotating-wave approximation [39]. We come back to the Hamiltonian in Eq. (1) and apply a unitary transformation with respect to

$$S(t) = \exp\left\{i\frac{\Omega_R(t)}{\omega_a + \omega_b(t)}\sin[\Omega_b(t) + \varphi_R(t)]\sigma_x\right\}. \quad (3)$$

The original Hamiltonian in the interaction picture is

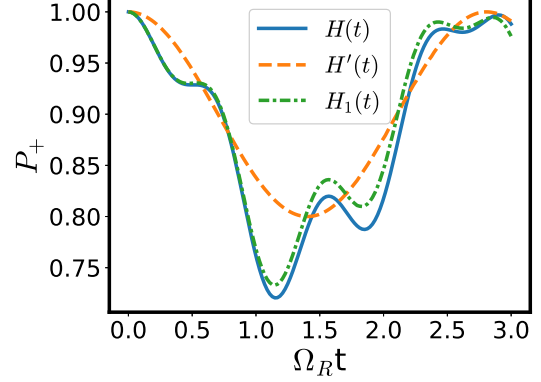


FIG. 1. The population dynamics of the qubit on  $|+\rangle$  under various Hamiltonians, in units of the Rabi frequency  $\Omega_R$ . The parameters are set as  $\omega_a = 100\pi$  MHz,  $\omega_b = 60\pi$  MHz, and  $\Omega_R = 20\pi$  MHz.

then rewritten as

$$\begin{aligned} H_0(t) &= S(t)H(t)S^\dagger(t) + i\dot{S}(t)S^\dagger(t) \\ &= \frac{\omega_a}{2}\sigma_z + \Omega_R(t)\cos[\Omega_b(t) + \varphi_R(t)]\sigma_x \\ &\quad + \frac{\Omega_R(t)\omega_a}{\omega_a + \omega_b(t)}\sin[\Omega_b(t) + \varphi_R(t)]\sigma_y + \mathcal{O}(\Omega_R^2) \\ &\quad - \frac{d}{dt}\left\{\frac{\Omega_R(t)}{\omega_a + \omega_b(t)}\sin[\Omega_b(t) + \varphi_R(t)]\sigma_x\right\} \\ &\approx \frac{\omega_a}{2}\sigma_z + \frac{\Omega_R(t)\omega_a}{\omega_a + \omega_b(t)}\left[e^{-i\Omega_b(t)-i\varphi_R(t)}\sigma_+ + h.c.\right], \end{aligned} \quad (4)$$

where we omitted the contribution up to the second-order of  $\mathcal{O}(\Omega_R^2)$  and the first-order derivative of the driving parameters with respect to time [14, 34] under the assumptions that  $|\dot{\omega}_b(t)|$ ,  $|\dot{\varphi}_R(t)|$ ,  $|\dot{\Omega}_R(t)| \ll |\omega_a + \omega_b(t)|$ .

Subsequently in the rotating frame with respect to  $R(t)$ , one can find a standard time-modulated Hamiltonian describing a qubit under a 3D effective magnetic field, i.e.,

$$\begin{aligned} H_1(t) &= \frac{\vec{B}(t)}{2} \cdot \vec{\sigma} = \frac{B_0(t)}{2}\vec{n}(t) \cdot \vec{\sigma} \\ &= \frac{\Omega_R(t)\omega_a}{\omega_a + \omega_b(t)}[\cos\varphi_R(t)\sigma_x + \sin\varphi_R(t)\sigma_y] \\ &\quad + \frac{\omega_a - \omega_b(t)}{2}\sigma_z, \end{aligned} \quad (5)$$

where  $\vec{n}(t) \equiv [\sin\theta(t)\cos\phi(t), \sin\theta(t)\sin\phi(t), \cos\theta(t)]$  parameterizes the direction of the magnetic field and  $\vec{\sigma}$  represents the vector of Pauli operators. Using the driving parameters, we have

$$\begin{cases} B_0(t) = \sqrt{[\omega_a - \omega_b(t)]^2 + \left[\frac{2\Omega_R(t)\omega_a}{\omega_a + \omega_b(t)}\right]^2}, \\ \phi(t) = \varphi_R(t), \\ \theta(t) = \arctan\left[\frac{2\Omega_R(t)\omega_a}{\omega_a^2 - \omega_b^2(t)}\right], \end{cases} \quad (6)$$

The Hamiltonian in Eq. (5) adapts to a larger Rabi frequency  $\Omega_R$  than that in Eq. (2) by holding the first-order contribution from the counter-rotating interaction. The distinction between these two approximated Hamiltonians can be transparently illustrated by the dynamics of Rabi oscillation, when the magnitudes of  $\omega_a$ ,  $\omega_b$ , and  $\Omega_R$  are chosen in almost the same order. In Fig. 1, we present the population dynamics of a two-level system, which is prepared as  $|+\rangle = (1, 0)^T$ , respectively under the original Hamiltonian  $H(t)$  in Eq. (1), the RWA Hamiltonian  $H'(t)$  in Eq. (2), and the modified RWA Hamiltonian  $H_1(t)$  in Eq. (5). Much to our anticipation, the rotating-wave interaction captures a sinusoid behavior in quality, while losing almost all the details of the dynamics. In contrast, with the aid of the unitary transformation  $S(t)$  in Eq. (3), the analytical result by  $H_1(t)$  is highly close to the numerical one by the original Hamiltonian  $H(t)$ .

We then apply the transformed Hamiltonian  $H_1(t)$  to build a more accurate quantum gate out of the regime of RWA. A universal set of single-qubit gate can be implemented by virtue of the time-dependent  $\theta(t)$  and  $\phi(t)$  in Eq. (6).  $B_0$  is set as a constant number for simplicity. To avoid the undesired transition between the instantaneous eigenstates of  $H_1(t)$  with accelerated time-dependence, one can add a counterdiabatic term following the transitionless quantum driving [20] approach. The ancillary Hamiltonian  $H_{\text{CD}}(t)$  can be expressed by

$$\begin{aligned} H_{\text{CD}}(t) &= \frac{1}{2}[\vec{n}(t) \times \partial_t \vec{n}(t)] \cdot \vec{\sigma} \\ &= \frac{1}{2}(-\dot{\theta} \sin \phi - \dot{\phi} \sin \theta \cos \theta \cos \phi, \\ &\quad \dot{\theta} \cos \phi - \dot{\phi} \sin \theta \cos \theta \sin \phi, \dot{\phi} \sin^2 \theta) \cdot \vec{\sigma}, \end{aligned} \quad (7)$$

where  $\vec{n}(t)$  is the unit vector of the magnetic field in Eq. (5). In Eq. (7), the explicit  $t$ -dependence of quantities has been omitted for simplicity, i.e.,  $\theta \equiv \theta(t)$  and  $\phi \equiv \phi(t)$ . The corrected Hamiltonian with the counterdiabatic term is  $H_{\text{tot}}(t) = H_1(t) + H_{\text{CD}}(t)$ , which could be diagonalized with the unitary transformation  $U_0(t) = \exp(i\theta\sigma_y/2) \exp(i\phi\sigma_z/2)$ :

$$\begin{aligned} H_z(t) &= U_0(t) H_{\text{tot}}(t) U_0^\dagger(t) + i\dot{U}_0(t) U_0^\dagger(t) \\ &= \frac{1}{2}(B_0 - \dot{\phi} \cos \theta) \sigma_z. \end{aligned} \quad (8)$$

The time-evolution operator  $U(t)$  in the lab frame can be obtained by

$$\begin{aligned} U(t) &= U_0^\dagger(t) U_R(t) = e^{-i\phi\sigma_z/2} e^{-i\theta\sigma_y/2} e^{-i \int_0^t ds H_z(s)} \\ &= \begin{pmatrix} \cos \frac{\theta(t)}{2} e^{-\frac{i}{2}[\alpha(t) + \phi(t)]} & -i \sin \frac{\theta(t)}{2} e^{\frac{i}{2}[\alpha(t) - \phi(t)]} \\ i \sin \frac{\theta(t)}{2} e^{-\frac{i}{2}[\alpha(t) - \phi(t)]} & \cos \frac{\theta(t)}{2} e^{\frac{i}{2}[\alpha(t) + \phi(t)]} \end{pmatrix}, \end{aligned} \quad (9)$$

where  $\alpha(t) = \int_0^t ds (B_0 - \dot{\phi} \cos \theta)$ . Under a proper boundary condition,  $U(t)$  can be used to realize any desired rotation or qubit-gate. For example, when  $\theta(T) = \pi$  and  $\alpha(T) - \phi(T) = \pi$  is satisfied,  $U(T)$  can realize a Pauli-X

gate. In the following discussion, we are concerned with the phase shift in a cyclic evolution. With  $\theta(T) = 2\pi$ , the final time-evolution operator is found to be in a diagonal form:

$$U(T) = \begin{pmatrix} e^{-\frac{i}{2}[\alpha(T) + \phi(T)]} & 0 \\ 0 & e^{\frac{i}{2}[\alpha(T) + \phi(T)]} \end{pmatrix}, \quad (10)$$

up to an unobservable global  $\pi$ -phase. In particular, when  $|\psi(0)\rangle = |\pm\rangle$ , one can derive a cyclic process  $|\psi(T)\rangle = e^{i\pi \mp \frac{i}{2}[\alpha(T) + \phi(T)]} |\psi(0)\rangle = e^{i(\pi \mp \gamma_{\pm})} |\psi(0)\rangle$ . The total phase accumulated in this period is

$$\gamma_{\pm} = \mp \frac{1}{2} \int_0^T dt [B_0 - \dot{\phi}(\cos \theta - 1)]. \quad (11)$$

The dynamical phase could be obtained by the corrected Hamiltonian  $H_{\text{tot}}(t)$  and the eigenstates of the effective Hamiltonian  $H_1(t)$ . In the lab frame, we have

$$\begin{aligned} \gamma_{\pm}^d &\equiv - \int_0^T dt \langle \psi(t) | H_{\text{tot}}(t) | \psi(t) \rangle \\ &= - \int_0^T dt \langle \pm | U_0(t) H_{\text{tot}}(t) U_0^\dagger(t) | \pm \rangle \\ &= - \int_0^T dt \langle \pm | \frac{1}{2}(-\dot{\phi} \sin \theta \sigma_x + \dot{\theta} \sigma_y + B_0 \sigma_z) | \pm \rangle \\ &= \mp \frac{1}{2} \int_0^T dt B_0 = \mp \frac{1}{2} B_0 T. \end{aligned} \quad (12)$$

The geometric phase is thus given by

$$\gamma_{\pm}^g = \gamma_{\pm} - \gamma_{\pm}^d = \mp \frac{1}{2} \int_0^T dt \dot{\phi}(1 - \cos \theta), \quad (13)$$

which is exactly the solid angle in the Bloch sphere described by  $\theta$  and  $\phi$  up to a scale of  $-1/2$  [40]. The evolution period  $T$  could be shortened by TQD as long as the boundary conditions are satisfied.

Provided that the dynamical phase is completely cancelled by any control technique, such as the dynamical decoupling [19, 41] to be discussed later, the geometric phase in Eq. (13) determines the final time evolution operator:

$$U(T) \simeq \begin{pmatrix} e^{i\gamma_{+}^g} & 0 \\ 0 & e^{i\gamma_{-}^g} \end{pmatrix} \simeq \begin{pmatrix} 1 & 0 \\ 0 & e^{i \int_0^T dt \dot{\phi}(1 - \cos \theta)} \end{pmatrix}. \quad (14)$$

Then we can build a quantum geometric phase gate. Under the assumption  $\theta(t) = \omega t$ , the period is  $T = 2\pi/\omega$  and  $U(t) = \text{diag}\{1, e^{i\eta}\}$ , where  $\eta = \gamma_{-}^g - \gamma_{+}^g$ . Arbitrary phase gate could be attained by adjusting  $\phi$ . For example, we can have a Pauli-Z when  $\phi = \omega t/2$  and we have a  $\pi/2$  gate when  $\phi = \omega t/4$ . In general, an arbitrary input state  $|\psi(0)\rangle = \cos \alpha_1 |+\rangle + \sin \alpha_1 e^{i\alpha_2} |-\rangle$  would be transformed by the phase-gate to

$$|\psi(T)\rangle = \cos \alpha_1 |+\rangle + \sin \alpha_1 e^{i\alpha_2} e^{i\eta} |-\rangle \quad (15)$$

where  $\alpha_1$  and  $\alpha_2$  are real-number angles with  $\{\alpha_1, \alpha_2\} \in [0, 2\pi]$ .

### III. THE EFFECTS FROM CLASSICAL NOISE

The geometric transformation in Eq. (15), which has been accelerated by the counterdiabatic protocol, cannot be faithfully realized in the presence of nonideal driving. The existence of the classical noise gives rise to the deviation of the gate-fidelity. Here we demonstrate how the noises on various control parameters would be detrimental to the performance of quantum gates in the absence of dynamical decoupling. Then in this section, we temporarily include the dynamical phase in Eq. (12) that is exclusively determined by  $B_0$ .  $\eta = \gamma_-^g - \gamma_+^g$  in Eq. (15) becomes  $\eta = \gamma_- - \gamma_+$ , i.e.,

$$\eta = \int_0^T dt \left[ B_0 - \dot{\phi}(\cos \theta - 1) \right]. \quad (16)$$

To measure the phase deviation by the classical noise on the quantum gate, we use a gate-fidelity [25, 42, 43] defined as

$$\mathcal{F} = \frac{1}{4\pi^2} \int_0^{2\pi} d\alpha_1 \int_0^{2\pi} d\alpha_2 \frac{M[\langle +|\rho(T)|-\rangle]}{\langle +|\psi(T)\rangle\langle\psi(T)|-\rangle}, \quad (17)$$

where  $\rho(t)$  is the time-evolved density matrix under the stochastic noise and the denominator is obtained by Eq. (15). It is clear that  $\mathcal{F}$  results from the ensemble average over both the random realizations of fluctuations in control parameters, e.g.,  $B_0 \rightarrow B_0 + \delta_B(t)$ , and the arbitrary input states characterized by  $\alpha_1$  and  $\alpha_2$ .

In this work, the stationary Gaussian noise [25, 44]  $\delta_\xi(t)$  is assumed to follow the statistical properties of

$$\langle \delta_\xi(t) \rangle = 0, \quad C(t-s) = \langle \delta_\xi(t) \delta_\xi(s) \rangle = \frac{\Gamma\gamma}{2} e^{-\gamma|t-s|}, \quad (18)$$

where the subscript  $\xi$  indicates the noise source,  $\Gamma$  is the correlation intensity of the noise, and  $\gamma$  is the memory parameter. The Fourier transform of the two-point correlation function  $C(t-s)$  gives rise to an inverse-quadratic spectral density,

$$S(\omega) = \int_{-\infty}^{\infty} dt e^{i\omega t} C(t) = \frac{2\Gamma\gamma^2}{\omega^2 + \gamma^2}. \quad (19)$$

When  $\gamma \rightarrow \infty$ ,  $S(\omega)$  becomes structureless and describes a Markovian or white noise; while when  $\gamma \rightarrow 0$ , it describes a typical non-Markovian noise with a finite-memory capability. In the following, we calculate the gate-fidelity during the free induction decay under the parametric fluctuations associated respectively with the magnetic field intensity  $B_0$  and the phase  $\phi$ . Note these two parameters are separable in the expression of quantum phase, allowing the individual analysis over different resource of noise.

#### A. Fidelity under noisy magnetic field intensity

We first consider a fluctuated magnetic field  $B_0$  in constructing the phase gate, which is determined by the driving parameters in Eq. (5). With respect to the unitary

transformation  $U_0(t)$ , the nonideal counterdiabatic corrected Hamiltonian in Eq. (8) becomes

$$\tilde{H}_z(t) = \frac{1}{2} \left[ B_0 + \delta_B(t) - \dot{\phi} \cos \theta \right] \sigma_z. \quad (20)$$

Consequently, the off-diagonal term of the final density matrix can be obtained by

$$\langle +|\rho(T)|-\rangle = \left\langle + \left| e^{-i \int_0^T dt \tilde{H}_z(t)} \rho(0) e^{i \int_0^T dt \tilde{H}_z(t)} \right| - \right\rangle \quad (21)$$

where  $\rho(0) \equiv |\psi(0)\rangle\langle\psi(0)|$ . Then we have

$$\frac{\langle +|\rho(T)|-\rangle}{\langle +|\psi(T)\rangle\langle\psi(T)|-\rangle} = \exp \left[ -i \int_0^T dt \delta_B(t) \right]. \quad (22)$$

Note that this result is independent of  $\alpha_1$  and  $\alpha_2$ , meaning that the noise effect on the gate-fidelity does not rely on the input states. Substituting it into Eq. (17) and using the statistical properties in Eq. (18), we have [32]

$$\mathcal{F}_B = e^{-\frac{1}{2} \int_0^T dt \int_0^T ds C(t-s)} = e^{-\frac{\Gamma}{2\gamma} (\gamma T + e^{-\gamma T} - 1)}. \quad (23)$$

The dependence of the gate-fidelity  $\mathcal{F}_B$  on the dimensionless cyclic period  $\gamma T$  and the memory parameter  $\Gamma/\gamma$  is plotted in Fig. 2.

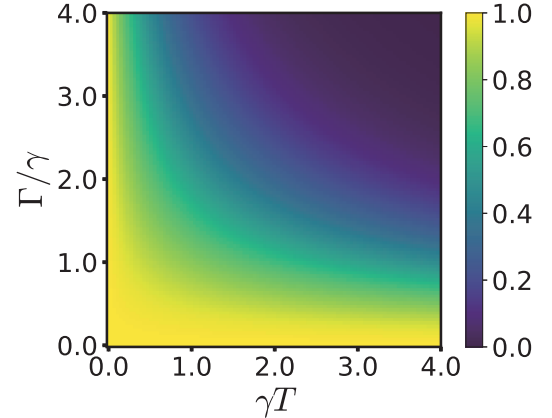


FIG. 2. Landscape of the gate-fidelity  $\mathcal{F}_B$  under the stochastic  $B_0$  in the parameter space of the strength-memory ratio  $\Gamma/\gamma$  and the running period  $\gamma T$ .

From both Eq. (23) and Fig. 2, a sufficiently large  $\Gamma/\gamma$  or a sufficiently small  $\gamma$  gives rise to a nearly exponential decay, which is consistent with a dynamics following a conventional Markovian decoherence raised by a white noise. While the non-exponential decay appears in the short-time regime with  $\gamma T \ll 1$ , where up to the leading order the exponent of the fidelity in Eq. (23) becomes quadratic to the running time:

$$\mathcal{F}_B \approx \exp \left( -\frac{\Gamma\gamma}{4} T^2 \right). \quad (24)$$

Then we can obtain the characteristic decoherence time  $T_2$  by the definition  $\ln \mathcal{F}_B(T_2) = -1$  [42]

$$T_2 = \frac{2}{(\Gamma\gamma)^{1/2}} \quad (25)$$

for the free induction decay. Clearly the gate-fidelity can be maintained at a high-level in the presence of a weak and non-Markovian classical noise. It is found when  $\Gamma/\gamma \leq 1.0$ ,  $\mathcal{F}_B$  is over 0.90 at  $\gamma T = 0.72$ .

### B. Fidelity under noisy control phase $\phi$

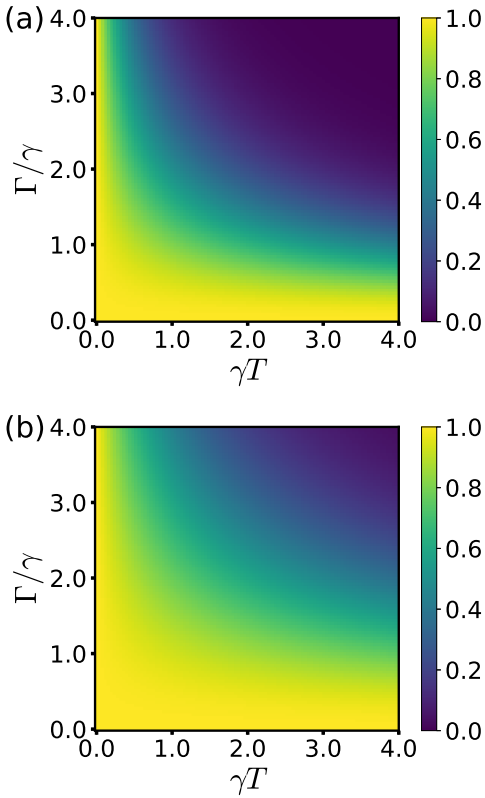


FIG. 3. Landscape of the gate-fidelity  $\mathcal{F}_\phi$  under the stochastic  $\phi$  in the parameter space of the strength-memory ratio  $\Gamma/\gamma$  and the running period  $\gamma T$ . In (a) and (b), the noise-free parameter  $\theta$  is set as  $\theta(t) = \omega t$  and  $\theta(t) = \omega t - \sin(\omega t)$ , respectively.

Now we consider that the control over the phase  $\phi$  is imperfect in the presence of random noises associated with its time-derivative  $\dot{\phi}$ , which lead to  $\phi(T) \rightarrow \phi(T) + \Delta_\phi(T)$  with  $\Delta_\phi(T) = \int_0^T dt \delta_\phi(t)$ . Then in the rotating frame, the nonideal Hamiltonian for the accelerated phase gate becomes,

$$\tilde{H}_z(t) = \frac{1}{2} \left\{ B_0 - [\dot{\phi} + \delta_\phi(t)] \cos \theta \right\} \sigma_z. \quad (26)$$

Using Eqs. (17), (21), and (26), it is straightforward to find for  $\theta = \omega t$  that

$$\begin{aligned} \mathcal{F}_\phi &= e^{-\frac{1}{2} \int_0^T dt \int_0^T ds [1 - \cos \theta(t)] [1 - \cos \theta(s)] C(t-s)} \\ &= \exp \left\{ -\frac{\Gamma}{4\gamma(4\pi^2 + \gamma^2 T^2)^2} [32\pi^4 e^{-\gamma T} \right. \\ &\quad \left. + 32\pi^4 (-1 + \gamma T) + 20\pi^2 (\gamma T)^3 + 3 (\gamma T)^5] \right\}, \end{aligned} \quad (27)$$

Similar to  $\mathcal{F}_B$  in Eq. (23), the fidelity  $\mathcal{F}_\phi$  in Eq. (27) is also the function of dimensionless parameters  $\gamma T$  and  $\Gamma/\gamma$ . An interesting observation is that under the short-running-time limit, i.e.,  $\gamma T \ll 1$ , we have  $\mathcal{F}_\phi \approx \exp(-\Gamma\gamma T^2/4)$ , the same as that in Eq. (24). Then we obtain the same decoherence timescale  $T_2$  as in Eq. (25). In fact, one can hardly distinguish Fig. 2 and Fig. 3(a). It is found when  $\Gamma/\gamma \leq 1.0$ ,  $\mathcal{F}_\phi$  is over 0.90 at  $\gamma T = 0.69$ .

However, Eq. (27) is reminiscent of an improved scheme in construction of the quantum phase-gate by virtue of the flexibility of the time-dependence of  $\theta$ . Rather than a constant  $\theta$  used in the previous literature [19, 41], one can reduce the magnitude of the integrand in Eq. (27) by selecting a proper and experimentally accessible  $\theta(t)$ , provided that the boundary condition is satisfied. For the exponent of the fidelity in Eq. (27), the main contribution to the integral is around  $t - s \approx 0$  according to the exponential-decay behavior of the correlation function  $C(t - s)$  [see e.g., Eq. (18), and the monotonic or asymptotic decay behavior is popular for all the stationary Gaussian noises]. Then we have

$$\begin{aligned} &\int_0^T dt \int_0^T ds [1 - \cos \theta(t)] [1 - \cos \theta(s)] C(t-s) \\ &\propto \left\{ \int_0^T dt [1 - \cos \theta(t)] \right\}^2. \end{aligned}$$

The fidelity can thus be enhanced by reducing the magnitude of the integral  $\int_0^T dt [1 - \cos \theta(t)]$ . For example, one can replace  $\theta(t) = \omega t$  with  $\theta(t) = \omega t - \sin(\omega t)$  while holding the same boundary condition. The induced improvement in gate-fidelity can be observed in Fig. 3(b). In contrast to Fig. 3(a), we then can maintain  $\mathcal{F}_\phi$  over 0.90 with  $\Gamma/\gamma = 3.1$  when  $\gamma T = 0.69$ . And when  $\Gamma/\gamma = 1.0$ , the same high-level fidelity can be sustained until  $\gamma T = 1.24$ .

### IV. SUPPRESS NOISE BY DYNAMICAL DECOUPLING

The noise analysis over both  $\delta_B$  and  $\delta_\phi$  renders the same second-order behavior in the running time under the short-time limit, as given by Eqs. (24) and (25). The decay of the gate-fidelity induced by the classical noise on the control parameters can be suppressed by a sequence of dynamical decoupling. As a developed technique, dynamical decoupling can extend the coherence time in many experiments. It has been generalized into various sequences of pulse to neutralize the influence of the

environmental noises [45]. Spin echo (SE) [46] presents the simplest as well as the original form in these pulse sequences, which consists of only one  $\pi$ -pulse in the middle of the time evolution besides the one performed in the end. Based on SE, the Carr-Purcell-Meiboom-Gill sequence (CPMG) [22, 47, 48] employs two or more  $\pi$ -pulses. In general, the  $n$ -pulse version of CPMG [22] can be described by a sequence of  $t_k = (k - 1/2)T/n$ ,  $k = 1, 2, \dots, n$ , that is obtained in the frequency domain. When the noise spectrum has a hard cutoff [24], i.e.,  $S(\omega) \sim \omega\Theta(\omega_c - \omega)$ , where  $\Theta(x)$  is the Heaviside step function [ $\Theta(x) = 1$  when  $x \geq 0$  and  $\Theta(x) = 0$  when  $x < 0$ ] or has an exponential-decay cutoff, i.e.,  $S(\omega) \sim \exp(-\omega/\omega_c)$ , the Uhrig dynamical-decoupling (UDD) sequence [23] is shown to be the most efficient scheme. It can reduce the decoherence rate down to the  $n$ th order of the running time by using  $n$  non-periodical pulses. In this section, we focus on the noise spectrum of the magnetic field  $\delta_B(t)$  following the inverse-quadratic power-law. It is shown that the CPMG sequence is the optimized choice. The analysis can be straightforwardly extended to the noisy  $\dot{\phi}$ .

### A. Spin echo on geometric phase

We choose SE as an example to illustrate the DD effect on the geometric phase, from which the other pulse sequences can be analysed in a similar way. The SE scheme is designed as a concatenated process of two piecewise segments, i.e.,  $0 \rightarrow t_f$  and  $t_f \rightarrow T$ , where  $t_f = T/2$ . A  $\pi$ -pulse is inserted at the moment  $t_f$  to switch the sign of the eigenstates in the lab frame. Another  $\pi$ -pulse is imposed on the system in the end of the whole passage to complete a cyclic process. Starting from the initial state  $|\psi(0)\rangle = |+\rangle$  and denoting the instantaneous eigenstates as  $|\pm(t)\rangle$ , the whole process can be described by the following expressions:

$$\begin{aligned} |\psi(0)\rangle &= |+\rangle \rightarrow |\psi(t_f - 0^+)\rangle = e^{i\bar{\gamma}_1} |+(t_f)\rangle \xrightarrow{\pi \text{ pulse}} \\ |\psi(t_f + 0^+)\rangle &= e^{i\bar{\gamma}_1} |-(t_f)\rangle \rightarrow \\ |\psi(T - 0^+)\rangle &= e^{i(\bar{\gamma}_1 + \bar{\gamma}_2)} |-(T)\rangle \xrightarrow{\pi \text{ pulse}} \\ |\psi(T)\rangle &= e^{i(\bar{\gamma}_1 + \bar{\gamma}_2)} |+(T)\rangle = e^{i(\pi + \bar{\gamma}_1 + \bar{\gamma}_2)} |+\rangle, \end{aligned} \quad (28)$$

where the boundary condition has been applied in the last equation.  $\bar{\gamma}_1$  and  $\bar{\gamma}_2$  represent the quantum phases generated in the first and the second segments, respectively. According to Eqs. (10), (11), and (20), these two nonideal phases turn out to be

$$\begin{aligned} \bar{\gamma}_1 &= -\frac{1}{2} \int_0^{T/2} dt \left[ B_0 + \delta_B(t) - \dot{\phi}'(\cos \theta' - 1) \right], \\ \bar{\gamma}_2 &= \frac{1}{2} \int_{T/2}^T dt \left[ B_0 + \delta_B(t) - \dot{\phi}'(\cos \theta' - 1) \right], \end{aligned} \quad (29)$$

where  $\phi' = \phi$  and  $\theta' = \theta$  during the first-half period  $t \in (0, t_f)$  and  $\phi' = -\phi$  and  $\theta' = \theta$  during the second-

half period  $t \in (t_f, T)$  due to the effect of spin echo. By Eq. (29), the ideal dynamical phase proportional to  $B_0$  vanishes in the end of the running while the geometric phase is accumulated to realize a geometric transformation and it holds the same form as in Eq. (13). When the initial state starts from  $|\psi(0)\rangle = |-\rangle$ , the sign of those phases in Eq. (29) is reversed and the SE scheme still works. However, the accumulation of the stochastic noise  $\delta_B(t)$  associated with the dynamical phase does not vanish during the two consecutive time-integrals.

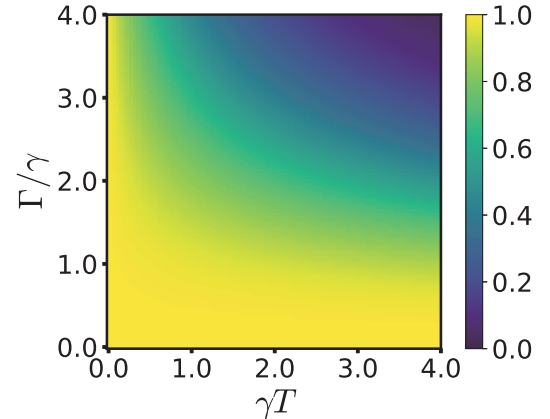


FIG. 4. Landscape of the spin-echo gate-fidelity  $\mathcal{F}_{\text{SE}}$  under the stochastic  $B_0$  in the parameter space of the strength-memory ratio  $\Gamma/\gamma$  and the running period  $\gamma T$ .

Then we measure the gate-fidelity in the presence of the random magnetic field under the spin echo scheme. The ratio of the off-diagonal elements of the density matrix in Eq. (17) is found to be

$$\frac{\langle +|\rho(T)|-\rangle}{\langle +|\psi(T)\rangle\langle\psi(T)|-\rangle} = e^{-i\left[\int_0^{T/2} dt \delta_B(t) - \int_{T/2}^T dt \delta_B(t)\right]}. \quad (30)$$

On ensemble average, we have

$$\begin{aligned} \mathcal{F}_{\text{SE}} &= M \left[ \exp \left( -i \int_0^{T/2} dt \delta_B(t) + i \int_{T/2}^T dt \delta_B(t) \right) \right] \\ &= \exp \left[ -\frac{\Gamma}{2\gamma} \left( \gamma T - e^{-\gamma T} - 3 + 4e^{-\gamma T/2} \right) \right], \end{aligned} \quad (31)$$

which is plotted in Eq. 4. In contrast to Fig. 2, one can find that under the SE scheme, the high-level regime of the gate-fidelity is significantly enlarged. When  $\Gamma/\gamma = 2.0$ ,  $\mathcal{F}_{\text{SE}}$  can be maintained over 0.98 for  $\gamma T = 1.0$ . In the short-time limit  $\gamma T \ll 1$ , we have

$$\mathcal{F}_{\text{SE}} \approx \exp \left( -\frac{\Gamma \gamma^2}{24} T^3 \right). \quad (32)$$

In contrast to the quadratic dependence Eq. (24), the exponent function is reduced to the third-order of the running time of the geometric gate by the spin echo effect.

We show in Appendix A that for the inversely quadratic power-law noise spectrum, one can further reduce the decay coefficient by more DD operations, yet cannot reduce the exponent function to more higher orders of the running interval  $T$ .

## B. CPMG on geometric phase

In general, we consider applying  $n$   $\pi$ -pulses into the running period  $(0, T)$  for constructing the geometric phase. The whole process is divided into  $n + 1$  segments described by  $0 \rightarrow t_1, t_1 \rightarrow t_2, \dots, t_n \rightarrow T$ . We now seek for an optimized sequence of the DD-operation moments  $t_k$ . Similar to Eq. (31), the gate-fidelity can be represented by

$$\mathcal{F}_n = M \left[ e^{-i \int_0^T dt \delta_B(t) f(T; t)} \right], \quad (33)$$

where  $f(T; t) = \sum_{k=0}^n (-1)^k \Theta(t_{k+1} - t) \Theta(t - t_k)$  with  $t_0 = 0$  and  $t_{n+1} = T$  and  $f(T; t)$  describes that the sign change of the quantum phase due to the switch between the eigenstates induced by the  $\pi$ -pulses. Moreover, to hold the same geometric phase as that in Eq. (13) for the FID process, the phase parameters  $\phi', \theta'$  in all the segments should be set as  $\phi' = f(T; t)\phi$  and  $\theta' = \theta$ .

The gate-fidelity in Eq. (33) can be represented by  $\mathcal{F}_n \equiv e^{-\chi(T)}$  [42, 43], where the decay function  $\chi(T)$  can be obtained by the noise spectrum  $S(\omega)$  and  $\tilde{f}(\omega, T) = \int_0^T dt e^{-i\omega t} f(T; t)$  [the Fourier transform of  $f(T; t)$ ],

$$\begin{aligned} \chi(T) &= \frac{1}{2} \int_{-\infty}^{\infty} \frac{d\omega}{2\pi} |\tilde{f}(\omega, T)|^2 S(\omega) \\ &= \frac{1}{2} \int_{-\infty}^{\infty} \frac{d\omega}{\pi} \frac{F(\omega T)}{\omega^2} S(\omega). \end{aligned} \quad (34)$$

Note in the second line of Eq. (34), a filter function  $F(\omega T) \equiv |\omega \tilde{f}(\omega, T)|^2/2$  is applied to measure the effects of the pulse sequence. Using the Taylor expansion around  $\omega T = 0$ , we have

$$\begin{aligned} \chi(T) &= \int_{-\infty}^{\infty} \frac{d\omega}{2\pi\omega^2} \left[ F(0) + F'(0)\omega T + F''(0) \frac{(\omega T)^2}{2!} \right. \\ &\quad \left. + F^{(3)}(0) \frac{(\omega T)^3}{3!} + \dots \right] S(\omega). \end{aligned} \quad (35)$$

Under the noise with a power-law spectrum  $S(\omega) \sim 1/\omega^m$ ,  $m \geq 2$ , the high-order terms  $F^{(n)}(0)$  with  $n - m \geq 1$  would lead to the nonconvergent integration  $\int_{-\infty}^{\infty} d\omega \omega^{n-2-m}$ . In contrast, if  $S(\omega)$  has a hard cutoff at an upper-bound  $\omega_c$  or has an exponential decay with frequency, such as  $S(\omega) \sim \exp(-\omega/\omega_c)$ , then the convergency could be held at any order. The UDD scheme [23] does not necessarily supply an optimized sequence for any polynomial spectrum.

Some existing works [42, 43] have addressed the noise  $\delta_B(t)$  with the statistical properties in Eq. (18). Here

we provide an alternative way to optimize the pulse sequence in the time domain for the quadratic power-law spectrum. In Appendix A, we find analytically the most efficient sequence can be described by

$$t_k = \frac{(k - 1/2)}{n} T, \quad k = 1, 2, \dots, n, \quad (36)$$

which is exactly the CPMG $n$  sequence with  $n \geq 2$ . When  $n = 1$ , it reduces to the SE sequence. When  $n = 2$ , it is also coincident to the UDD sequence.

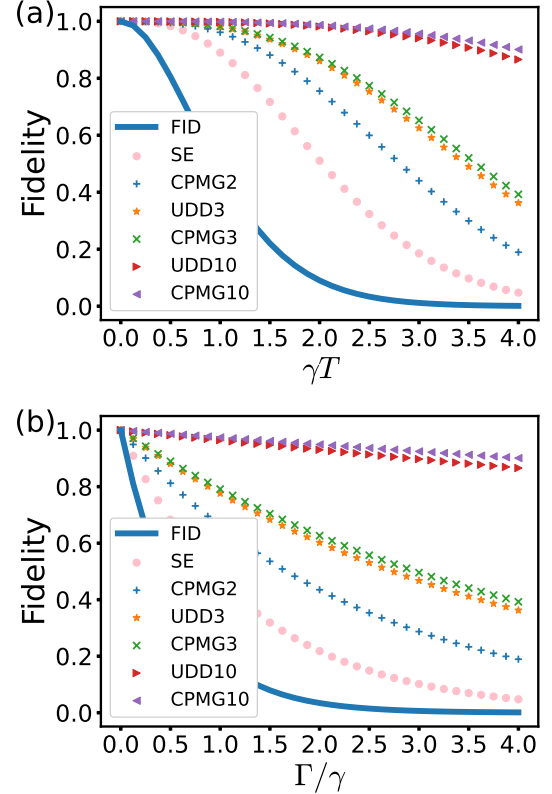


FIG. 5. The gate-fidelity under various DD sequences (SE, CPMG $n$ , and UDD $n$ ) in the presence of the Gaussian noise following the inverse-quadratic power-law spectrum. (a) the gate dynamics versus  $\gamma T$  when  $\Gamma/\gamma = 4$ ; (b) the gate dependence on  $\Gamma/\gamma$  when  $\gamma T = 4$ .

In Fig. 5, we show the gate-fidelity under various DD-sequence controls in terms of the dynamics and their dependence on the memory parameter. The solid line, circle-dotted line, plus-dotted line, star-dotted line, cross-dotted line, right-triangle-dotted line, and left-triangle-dotted line represent the fidelities under FID, SE, CPMG2, UDD3, CPMG3, UDD10, and CPMG10, respectively, where  $n$  denotes the number of  $\pi$ -pulses. In both Fig. 5(a) and Fig. 5(b), the performance of the geometric phase gate is steadily improved by inserting more periodical  $\pi$ -pulses into the running period. We also demonstrate that CPMG $n$  outperforms UDD $n$  when  $n \geq 3$ . It is found when  $\Gamma/\gamma = 4.0$  and  $\gamma T = 4.0$ , the gate-fidelity can be maintained over 0.90 by CPMG10.

By Eqs. (36) and (34), it is found up to the leading-order contribution, that the gate-fidelity becomes

$$\mathcal{F}_n \approx \exp \left[ -\frac{\Gamma}{24n^2\gamma} (\gamma T)^3 \right]. \quad (37)$$

As for the scale behavior of the characteristic time  $T_2$  over the pulse number  $n$ , we have

$$T_2 = \left( \frac{24}{\Gamma\gamma^2} \right)^{1/3} n^{2/3}. \quad (38)$$

The power-law with  $n^{2/3}$  implies to enhance the coherence time of our geometric phase gate by more DD pulses.

## V. CONCLUSIONS

In summary, we construct a quick-and-faith geometric phase gate by combining the transitionless-quantum-driving and the dynamical decoupling control into the Berry phase. The former technique is used to shorten the running time as required by the adiabatic passage and the latter is used to neutralize the classical noise on the control parameters. Our proposal is based on a semi-classical Rabi model describing the dynamics of a two-level atomic system under a parametric driving. Under a modified transformation holding the first-order contribution from the counter-rotating interaction, our method is superior to the conventional rotating-wave approximation and adapts to a strong driving out of the dispersive regime. We analysis the gate-fidelity under the random fluctuation or noise on the effective magnetic field and the control phase. In the time domain, we find that the CPMG $n$  sequence is the most efficient DD scheme under the inversely quadratic power-law noise to maintain a high-level fidelity and we obtain the scaling behavior of the decoherence time  $T_2$  with respect to the DD operation number  $n$ . Our investigation provides a systematic estimation over the errors in constructing the Berry-phase gate caused by the classical noise. It is expected to be useful for optimizing the performance of quantum gates under Gaussian noise following a power-law spectrum.

## ACKNOWLEDGMENTS

We acknowledge financial support from the National Science Foundation of China (Grants No. 11974311 and No. U1801661).

## Appendix A: Optimized sequence for Gaussian noise

This appendix contributes to finding an optimized DD sequence to cancel the classical Gaussian noise on the magnetic-field intensity. We provide a proof in the time domain rather than that in the frequency domain. The

calculation starts from the gate-fidelity under  $n$  pulses in Eq. (33). Using the correlation function in Eq. (18), we have

$$\begin{aligned} \mathcal{F}_n(\{t_k, k = 1, 2, \dots, n\}) &= M \left[ e^{-i \int_0^T dt \delta_B(t) f(T; t)} \right] \\ &= \exp \left[ -\frac{1}{2} \int_0^T dt \int_0^T ds C(t-s) f(T; t) f(T; s) \right]. \end{aligned} \quad (A1)$$

With the dimensionless parameters  $x \equiv \gamma T$ ,  $y \equiv \Gamma/\gamma$  and  $\mu_k \equiv t_k/T$ , the decay function  $\chi(x, y) \equiv -\ln \mathcal{F}_n$  can be expressed by

$$\begin{aligned} \chi(x, y) &= \frac{y}{2} \left[ x - 1 + (-1)^n e^{-x} \right. \\ &\quad \left. - 2 \sum_{k=0}^{n+1} \sum_{j=1}^n (-1)^{|k-j|} e^{-|\mu_k - \mu_j| x} \right], \end{aligned} \quad (A2)$$

where  $\mu_0 = 0$  and  $\mu_{n+1} = 1$ . Note expanding  $\chi(x, y)$  about  $x$  is equivalent to expanding it about  $T$ . It is obtained that

$$\chi(x, y) = \frac{y}{2} (C_0 + C_1 x + C_2 x^2 + C_3 x^3 + \dots), \quad (A3)$$

where the coefficients of the first leading orders are

$$C_0 = -1 + (-1)^n - 2 \sum_{k=0}^{n+1} \sum_{j=1}^n (-1)^{|k-j|}, \quad (A4a)$$

$$C_1 = 1 - (-1)^n + 2 \sum_{k=0}^{n+1} \sum_{j=1}^n (-1)^{|k-j|} |\mu_k - \mu_j|, \quad (A4b)$$

$$C_2 = \frac{1}{2} (-1)^n - \sum_{k=0}^{n+1} \sum_{j=1}^n (-1)^{|k-j|} |\mu_k - \mu_j|^2, \quad (A4c)$$

$$C_3 = \frac{1}{6} (-1)^{n+1} + \frac{1}{3} \sum_{k=0}^{n+1} \sum_{j=1}^n (-1)^{|k-j|} |\mu_k - \mu_j|^3. \quad (A4d)$$

It is straightforward to verify that both the zero-order and the first-order coefficients  $C_0$  and  $C_1$  are exactly 0, independent of the pulse sequence  $\{\mu_k\}$ . When  $n$  is an even integer, the summation in the second-order coefficient  $C_2$  can be decomposed into three terms, being relevant to  $\mu_k^2$ ,  $-2\mu_k\mu_j$ , and  $\mu_j^2$ , respectively. By virtue of  $\mu_0 = 0$  and  $\mu_{n+1} = 1$ , the first or the third term is proved to vanish by

$$\sum_{k=0}^{n+1} \sum_{j=1}^n (-1)^{|k-j|} \mu_k^2 = \sum_{k=0}^{n+1} \mu_k^2 \sum_{j=1}^n (-1)^{|k-j|} = 0. \quad (A5)$$

Equation (A4c) can then be reduced to

$$\begin{aligned}
C_2 &= \frac{1}{2} + 2 \sum_{k=0}^{n+1} \sum_{j=1}^n (-1)^{|k-j|} \mu_k \mu_j \\
&= \frac{1}{2} + 2 \left[ \sum_{k=1}^n (-1)^{k-1} \mu_k \right]^2 + 2 \sum_{k=1}^n (-1)^{k-1} \mu_k \quad (\text{A6}) \\
&= \frac{1}{2} \left[ 1 + \sum_{k=1}^n (-1)^{k-1} 2\mu_k \right]^2.
\end{aligned}$$

When  $n$  is odd, the summations about  $\mu_k^2$  and  $\mu_j^2$  in  $C_2$  are simplified to

$$\begin{aligned}
&\sum_{k=0}^{n+1} \mu_k^2 \sum_{j=1}^n (-1)^{|k-j|} + \sum_{j=1}^n \mu_j^2 \sum_{k=0}^{n+1} (-1)^{|k-j|} \\
&= \sum_{k=0}^{n+1} \mu_k^2 (-1)^{|k-1|} + \sum_{j=1}^n \mu_j^2 (-1)^j \\
&= \mu_0^2 (-1)^1 + \mu_{n+1}^2 (-1)^n = -1. \quad (\text{A7})
\end{aligned}$$

Then Eq. (A4c) can be reduced to

$$\begin{aligned}
C_2 &= -\frac{1}{2} - (-1) + 2 \sum_{k=0}^{n+1} \sum_{j=1}^n (-1)^{|k-j|} \mu_k \mu_j \\
&= \frac{1}{2} + 2 \left[ \sum_{k=1}^n (-1)^{k-1} \mu_k \right]^2 - 2 \sum_{k=1}^n (-1)^{k-1} \mu_k \quad (\text{A8}) \\
&= \frac{1}{2} \left[ -1 + \sum_{k=1}^n (-1)^{k-1} 2\mu_k \right]^2.
\end{aligned}$$

The condition of  $C_2 = 0$ , which can be summarized to

$$(-1)^n + 2 \sum_{k=1}^n (-1)^{k-1} \mu_k = 0, \quad (\text{A9})$$

has a clear physical meaning or consequence that after applying those  $\pi$ -pulses at  $\mu_k$ , the dynamical phase in the absence of noise is thus exactly eliminated to leave a geometric transformation. With  $C_2 = 0$  and the extreme-value condition  $\partial_{\mu_k} C_3 = 0$  under the constraints that  $0 < \mu_1 < \mu_2 < \dots < \mu_n < 1$ , we find the solution is exactly the CPMGn, i.e.,  $\mu_k = (k - 1/2)/n$ . And the minimum-value of the third-order coefficient  $C_3$  turns out to be  $x^3/(12n^2)$ , which corresponds to the decay behavior in Eq. (37) of the main text. The result also demonstrates that the  $C_3$  cannot be completely eliminated under arbitrary choice of  $\mu_k$  or  $t_k$ .

---

[1] P. W. Shor, *Polynomial-time algorithms for prime factorization and discrete logarithms on a quantum computer*, *SIAM J. Comput.* **26**, 1484 (1997).

[2] L. K. Grover, *Quantum mechanics helps in searching for a needle in a haystack*, *Phys. Rev. Lett.* **79**, 325 (1997).

[3] R. Babbush, P. J. Love, and A. Aspuru-Guzik, *Adiabatic quantum simulation of quantum chemistry*, *Sci Rep* **4**, 1 (2014).

[4] R. Gerritsma, G. Kirchmair, F. Zähringer, E. Solano, R. Blatt, and C. Roos, *Quantum simulation of the dirac equation*, *Nature* **463**, 68 (2010).

[5] I. D. Kivlichan, J. McClean, N. Wiebe, C. Gidney, A. Aspuru-Guzik, G. K.-L. Chan, and R. Babbush, *Quantum simulation of electronic structure with linear depth and connectivity*, *Phys. Rev. Lett.* **120**, 110501 (2018).

[6] R. Harper, S. T. Flammia, and J. J. Wallman, *Efficient learning of quantum noise*, *Nat. Phys.* **16**, 1184 (2020).

[7] C. Song, S.-B. Zheng, P. Zhang, et al., *Continuous-variable geometric phase and its manipulation for quantum computation in a superconducting circuit*, *Nat Commun* **8**, 1 (2017).

[8] M. V. Berry, *Quantal phase factors accompanying adiabatic changes*, *Proc. R. Soc. Lond. A* **392**, 45 (1984).

[9] Y. Aharonov and J. Anandan, *Phase change during a cyclic quantum evolution*, *Phys. Rev. Lett.* **58**, 1593 (1987).

[10] J. Samuel and R. Bhandari, *General setting for berry's phase*, *Phys. Rev. Lett.* **60**, 2339 (1988).

[11] F. Wilczek and A. Zee, *Appearance of gauge structure in simple dynamical systems*, *Phys. Rev. Lett.* **52**, 2111 (1984).

[12] J. Anandan, *Non-adiabatic non-abelian geometric phase*, *Phys. Lett. A* **133**, 171 (1988).

[13] D. Leibfried, B. DeMarco, V. Meyer, D. Lucas, M. Barrett, J. Britton, W. M. Itano, B. Jelenković, C. Langer, T. Rosenband, et al., *Experimental demonstration of a robust, high-fidelity geometric two ion-qubit phase gate*, *Nature* **422**, 412 (2003).

[14] J.-M. Cui, M.-Z. Ai, R. He, Z.-H. Qian, X.-K. Qin, Y.-F. Huang, Z.-W. Zhou, C.-F. Li, T. Tu, and G.-C. Guo, *Experimental demonstration of suppressing residual geometric dephasing*, *Sci. Bull.* **64**, 1757 (2019).

[15] J. A. Jones, V. Vedral, A. Ekert, and G. Castagnoli, *Geometric quantum computation using nuclear magnetic resonance*, *Nature* **403**, 869 (2000).

[16] G. Feng, G. Xu, and G. Long, *Experimental realization of nonadiabatic holonomic quantum computation*, *Phys. Rev. Lett.* **110**, 190501 (2013).

[17] A. A. Abdumalikov Jr, J. M. Fink, K. J. Julliussone, M. Pechal, S. Berger, A. Wallraff, and S. Filipp, *Experimental realization of non-abelian non-adiabatic geometric gates*, *Nature* **496**, 482 (2013).

[18] Y. Xu, W. Cai, Y. Ma, X. Mu, L. Hu, T. Chen, H. Wang, Y. P. Song, Z.-Y. Xue, Z.-q. Yin, and L. Sun,

*Single-loop realization of arbitrary nonadiabatic holonomic single-qubit quantum gates in a superconducting circuit*, *Phys. Rev. Lett.* **121**, 110501 (2018).

[19] X. B. Wang and M. Keiji, *Nonadiabatic conditional geometric phase shift with nmr*, *Phys. Rev. Lett.* **87**, 097901 (2001).

[20] M. V. Berry, *Transitionless quantum driving*, *J. Phys. A: Math. Theor.* **42**, 365303 (2009).

[21] L. Viola and S. Lloyd, *Dynamical suppression of decoherence in two-state quantum systems*, *Phys. Rev. A* **58**, 2733 (1998).

[22] W. M. Witzel and S. D. Sarma, *Multiple-pulse coherence enhancement of solid state spin qubits*, *Phys. Rev. Lett.* **98**, 077601 (2007).

[23] G. S. Uhrig, *Keeping a quantum bit alive by optimized  $\pi$ -pulse sequences*, *Phys. Rev. Lett.* **98**, 100504 (2007).

[24] S. Pasini and G. S. Uhrig, *Optimized dynamical decoupling for power-law noise spectra*, *Phys. Rev. A* **81**, 012309 (2010).

[25] X.-K. Qin, G.-C. Guo, and Z.-W. Zhou, *Suppressing the geometric dephasing of berry phase by using modified dynamical decoupling sequences*, *New J. Phys.* **19**, 013025 (2017).

[26] S.-L. Zhu and Z. D. Wang, *Unconventional geometric quantum computation*, *Phys. Rev. Lett.* **91**, 187902 (2003).

[27] J. Du, P. Zou, and Z. D. Wang, *Experimental implementation of high-fidelity unconventional geometric quantum gates using an nmr interferometer*, *Phys. Rev. A* **74**, 020302 (2006).

[28] Z. S. Wang, C. Wu, X.-L. Feng, L. C. Kwek, C. H. Lai, C. H. Oh, and V. Vedral, *Nonadiabatic geometric quantum computation*, *Phys. Rev. A* **76**, 044303 (2007).

[29] X.-L. Feng, C. Wu, H. Sun, and C. H. Oh, *Geometric entangling gates in decoherence-free subspaces with minimal requirements*, *Phys. Rev. Lett.* **103**, 200501 (2009).

[30] O. Oreshkov, T. A. Brun, and D. A. Lidar, *Fault-tolerant holonomic quantum computation*, *Phys. Rev. Lett.* **102**, 070502 (2009).

[31] O. Oreshkov, T. A. Brun, and D. A. Lidar, *Scheme for fault-tolerant holonomic computation on stabilizer codes*, *Phys. Rev. A* **80**, 022325 (2009).

[32] C. Gardiner, P. Zoller, and P. Zoller, *Quantum noise: a handbook of Markovian and non-Markovian quantum stochastic methods with applications to quantum optics* (Springer Science & Business Media, 2004).

[33] C. Gerry, P. Knight, and P. L. Knight, *Introductory quantum optics* (Cambridge university press, 2005).

[34] P. J. Leek, J. M. Fink, A. Blais, R. Bianchetti, M. Göppl, J. M. Gambetta, D. I. Schuster, L. Frunzio, R. J. Schoelkopf, and A. Wallraff, *Observation of berry's phase in a solid-state qubit*, *Science* **318**, 1889 (2007).

[35] H. Zheng, S. Y. Zhu, and M. S. Zubairy, *Quantum zeno and anti-zeno effects: Without the rotating-wave approximation*, *Phys. Rev. Lett.* **101**, 200404 (2008).

[36] C. Deng, F. Shen, S. Ashhab, and A. Lupascu, *Dynamics of a two-level system under strong driving: Quantum-gate optimization based on floquet theory*, *Phys. Rev. A* **94**, 032323 (2016).

[37] Z. Lü and H. Zheng, *Effects of counter-rotating interaction on driven tunneling dynamics: Coherent destruction of tunneling and bloch-siegert shift*, *Phys. Rev. A* **86**, 023831 (2012).

[38] J. Jing, Z.-G. Lü, and Z. Ficek, *Breakdown of the rotating-wave approximation in the description of entanglement of spin-anticorrelated states*, *Phys. Rev. A* **79**, 044305 (2009).

[39] Z. Lü and H. Zheng, *Effects of counter-rotating interaction on driven tunneling dynamics: Coherent destruction of tunneling and bloch-siegert shift*, *Phys. Rev. A* **86**, 023831 (2012).

[40] W. Dong, F. Zhuang, S. E. Economou, and E. Barnes, *Doubly geometric quantum control*, *PRX Quantum* **2**, 030333 (2021).

[41] A. Gregefalk and E. Sjöqvist, *Transitionless quantum driving in spin echo*, *Phys. Rev. Applied* **17**, 024012 (2022).

[42] L. Cywiński, R. M. Lutchyn, C. P. Nave, and S. Das Sarma, *How to enhance dephasing time in superconducting qubits*, *Phys. Rev. B* **77**, 174509 (2008).

[43] P. Szałkowski, G. Ramon, J. Krzywda, D. Kwiatkowski, and L. Cywiński, *Environmental noise spectroscopy with qubits subjected to dynamical decoupling*, *J. Phys.: Condens. Matter* **29**, 333001 (2017).

[44] J. Jing, C.-H. Lam, and L.-A. Wu, *Non-abelian holonomic transformation in the presence of classical noise*, *Phys. Rev. A* **95**, 012334 (2017).

[45] W. Yang, Z.-Y. Wang, and R.-B. Liu, *Preserving qubit coherence by dynamical decoupling*, *Front. Phys. China* **6**, 2 (2011).

[46] E. L. Hahn, *Spin echoes*, *Phys. Rev.* **80**, 580 (1950).

[47] H. Y. Carr and E. M. Purcell, *Effects of diffusion on free precession in nuclear magnetic resonance experiments*, *Phys. Rev.* **94**, 630 (1954).

[48] S. Meiboom and D. Gill, *Modified spin-echo method for measuring nuclear relaxation times*, *Rev. Sci. Instrum.* **29**, 688 (1958).